arXiv:1505.05830v4 [physics.gen-ph] 23 Mar 2016

Cartan's Supersymmetry and the violation of CP symmetry

Sadataka Furui
Graduate School of Teikyo University
2-17-12 Toyosatodai, Utsunomiya, 320-0003 Japan,
e-mail furui@umb.teikyo-u.ac.jp

March 24, 2016

Abstract

Cartan's supersymmetriy fixes couplings of two types of fermions ψ, ϕ and two types of vector fields x_i and $x_{i'}$, $(i = 1, 2, 3, 4)$. The electromagnetic interaction of leptons and quarks is expressed as ${}^t\psi \mathcal{C} x_i \psi$. In the case of coupling of leptons and quarks with W, we extend the coupling ${}^t\phi \mathcal{C} X \psi$ to ${}^t\phi \mathcal{C} X(1-\gamma_5)\psi$, where $X = x_i$ or ${x_i}'$, and unify the interactions in the form ${}^t\phi \mathcal{C} \bar{x}_i \psi + {}^t\phi \mathcal{C} \bar{x_i}' \mathcal{C} \psi$, where $\bar{x}_i$ implies appropriate x_i or $(-\gamma_5 x_i)$ is chosen. The γ_5 term induces in time component of $B^0 \to K^0\, J/\Psi$, K^0 with the $\bar{s}$ quark dominated by the small component, while in space components of $\bar{B}^0 \to \bar{K}^0\, J/\Psi$, $\bar{K}^0$ with the s quark dominated by the small component. This asymmetry could be the origin of the CP asymmetry in the $B^0 \to K^0\, J/\Psi$.

We apply the model to $B^0_{s(d)} \to D^-_{s(d)} D^+_{s(d)}$ decays and study violation of CP symmetry via interference of tree and penguin contributions, and observe that the asymmetry is weak consistent to the experiment.

1 Introduction

Violation of CP symmetry was observed in the difference of $B^0 \to K^0 + X$ decay and $\bar{B}^0 \to \bar{K}^0 + X$ decay, where data with X chosen to be J/Ψ or $\pi^{\pm}$ [1, 2]. In the experiment of producing $B^0, \bar{B}^0$ entangled state in the $\Upsilon(4S)$ resonance decay, conditions of B^0 or $\bar{B}^0$ decay into $\ell^+ X$ or $\ell^- X$ and another B^0 or $\bar{B}^0$ decay into $J/\Psi K^0$ or $J/\Psi \bar{K}^0$ were chosen.

We consider violation of CP symmetry or time reversal symmetry in the decay of B mesons observed in the difference of

$$B^0 \to B_+(\ell^- \nu_\ell + X, J/\Psi \bar{K}_L^0) \text{ v.s. } \bar{B}^0 \to B_-(\ell^+ \nu_\ell + X, J/\Psi K_L^0).$$

where K_S^0 and K_L^0 are linear combinations of K^0 and $\bar{K}^0$,

$$|K_S^0\rangle = \mathcal{N}(p_k|K^0\rangle - q_k|\bar{K}^0\rangle)$$
$$|K_L^0\rangle = \mathcal{N}(p_k|K^0\rangle + q_k|\bar{K}^0\rangle),$$

where $\mathcal{N} = 1/\sqrt{p_k^2 + q_k^2}$.

From the difference of experimental data of

$$B^0 \to \pi^- K^+ \text{ v.s. } \bar{B}^0 \to \pi^+ K^-$$

one can evaluate the CKM angle γ and CP violation[3, 4], but we do not take this approach, since an entangled neutral B meson state $\Upsilon(4S)$ affects the phase γ[1].

Cartan's supersymmetry[5] defines the interaction of spinors (quarks or anti-quarks in B^0 meson) and vector particles (W, Z bosons or γ particles). In our application of the model to the electro-magnetic decay of a Higgs particle ($H^0 \to \gamma\gamma$) and weak decay ($H^0 \to W\bar{W}$) [6, 7, 8, 9] suggest that the quark-gluon and the quark-photon interaction of Cartan's supersymmetry could give clear signal of violation of the CP symmetry. In the standard model, CP symmetry violation occurs from the interference of the tree diagram amplitude and the penguin diagram amplitude[2]. Typical tree diagrams and penguin diagrams of this decay are shown in Fig.1 and Fig.2.

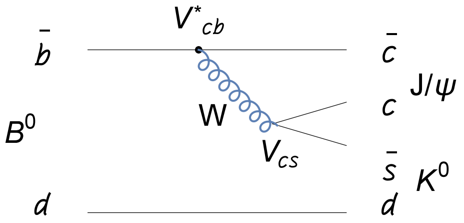

Figure 1: Typical tree diagram of $B^0 \to K_L^0\, J/\Psi$ decay. V_{cb} and V_{cs} are CKM amplitudes.

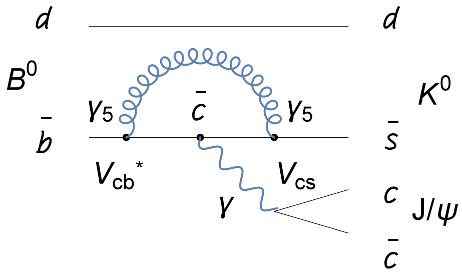

Figure 2: Typical penguin diagram of $B^0 \to K_L^0\, J/\Psi$ decay. In our model we include the loop of γs in addition to that of W bosons.

The decay rates of $\bar{B}^0(B^0) \to f$ is parametrized as

$$\Gamma_{\bar{B}^0(B^0)\to f} \propto e^{-\Gamma|\Delta t|}\{1+(-)[S_f\sin(\Delta m_d \Delta t) - C_f \cos(\Delta m_d \Delta t)]\},$$

where $\Delta t = t_{CP} - t_{flavor}$ is the difference of the decay time to the CP eigenstates and the decay time to the flavor eigenstates, and Δm_d is the mass difference between the physical states of the neutral B meson systems. The decay time difference Δt is approximately given by the distance Δd between the decay points and the Lorentz boost $\beta\gamma$ as $\Delta t \simeq \Delta d/\beta\gamma c$.

Adopting the parametrization of the low mass eigenstate B_L and the high mass eigenstate B_H as

$$\begin{aligned}|B_L\rangle &\propto p\sqrt{1-z}|B^0\rangle - q\sqrt{1+z}|\bar{B}^0\rangle \\ |B_H\rangle &\propto p\sqrt{1+z}|B^0\rangle + q\sqrt{1-z}|\bar{B}^0\rangle,\end{aligned}$$

where $|q/p| = 1$ and $z = 0$, if symmetry holds. The amplitude S_f and C_f are parametrized as

$$S_f = 2Im\lambda_f/(1+|\lambda_f|^2), \quad C_f = (1-|\lambda_f|^2)/(1+|\lambda_f|^2),$$

where using the CP parity $\eta_f = -1(+1)$ for $f = J/\Psi K_S^0(J/\Psi K_L^0)$ and

$$\lambda_f = \eta_f(q/p)(\bar{A}_f/A_f)(p_K/q_k).$$

Here $\bar{A}_f/A_f$ is the ratio of the $\bar{B}^0 \to f$ and $B^0 \to f$ decays.

Experimentally, violation of CP or time reversal symmetry can be observed via difference of Δt dependence of B^0 tagged events and $\bar{B}^0$ tagged events[1, 2]. The difference of B^0 tagged events and $\bar{B}^0$ tagged events shows the direction of the time axis[10].

The propagator between vertices V_{cb}^* and V_{cs} is assigned as a W boson, and the source of $c\bar{c}$ in the penguin diagram is assigned as a γ photon or Z boson. In our model, a γ particle A_μ is emitted from a quark in B^0 or $\bar{B}^0$ as

$$\bar{\psi}_L(\gamma_\mu(i\partial_\mu - e\,A_\mu) - m)\psi_L.$$

The quark ψ_L which consists of ψ and its small component $\mathcal{C}\psi$ interacts with an anti-quark ϕ_L which consists of ϕ and its small component $\mathcal{C}\phi$. A γ particle A_μ is emitted also from ϕ_L as

$$\bar{\phi}_L(\gamma_\mu(i\partial_\mu - e\,A_\mu) - m)\phi_L.$$

In the $SU(2) \times U(1)$ theory, A_μ, Z_μ and W_μ are related to the gauge fields A'_μ and B'_μ by

$$\begin{aligned} A_\mu &= \sin\theta_W {A'_\mu}^3 + \cos\theta_W B'_\mu \\ Z_\mu &= \cos\theta_W {A'_\mu}^3 - \sin\theta_W B'_\mu \\ W_\mu^\pm &= ({A'_\mu}^1 \mp i{A'_\mu}^2)/\sqrt{2}, \end{aligned}$$

where θ_W is the Weinberg angle.

In the standard model, the weak interaction is described as[11]

$$\begin{aligned} &\bar{\psi}_L^k\gamma_\mu(i\partial_\mu + g_2\frac{\tau^a}{2}W^a_{0\,\mu} + g_1\frac{y_k}{2}B_\mu)\psi_L^k \\ &+\bar{a}_R^k\gamma^\mu(i\partial_\mu + g_1\frac{1+y_k}{2}B_\mu)a_R^k \\ &+\bar{b}_R^k\gamma^\mu(i\partial_\mu + g_1\frac{-1+y_k}{2}B_\mu)b_R^k, \end{aligned} \tag{1}$$

where a_R^k and b_R^k are right-handed spinors. The weak isospin of quarks or leptons are defined by y^k. The isospin of W_0^a and B_μ are rotated, and physical states W_μ, A_μ, Z_μ and ψ_L appear. We expect that physical ϕ_L appear together with the physical ψ_L.

The Cabibbo-Kobayashi-Maskawa (CKM) amplitudes V_{cs}, V_{cb}, V_{cd} are parametrized as

$$\begin{aligned} V_{cs} &= 1-\frac{1}{2}\lambda^2-\frac{1}{8}\lambda^4(1+4A^2) \\ V_{cb} &= A\lambda^2 \\ V_{cd} &= -\lambda+\frac{1}{2}A^2\lambda^5[1-2(\rho+i\eta)] \end{aligned}$$

where $\lambda \simeq 0.23$.

Large $V_{cs} = 0.973$ yields strong $B^0(\bar{B}^0) \to K^0 + X(\bar{K}^0 + X)$ decay modes. The decay mode $B^0(\bar{B}^0) \to D^{*-}\ell^+\nu_\ell(D^{*+}\ell^-\nu_\ell)$ is strong due to relatively large $V_{cd} = 0.225$ and small $V_{ub} = 0.00355$ and $V_{cb} = 0.0414$. The relation $V_{cb} = A\lambda^2 = 0.0414$ requires $A = 0.78$, while $V_{cs} = 0.973$ requires $A = 0.38$, and the parametrization of the CKM amplitudes are not completed. We study also the decay of $B^0(\bar{B}^0) \to D^+D^-$ and $B_s(\bar{B}_s) \to D_s^+D_s^-$.

In section 2, we explain Cartan's supersymmetry in $B^0 \to K^0\, J/\Psi$ interaction, and in section3, we explain differences of $B^0 \to D^+D^-$ and $B_s \to D_s^+D_s^-$ from Cartan's supersymmetry.

2 Cartan's supersymmetry and weak interactions

We want to reproduce the qualitative features of CKM amplitudes from the trialty model. In the previous work[8], we could understand absence of $B_s(0^+)^+ \to B_s(0^-)\pi^+$, and presence of $B_s(0^+)^+ \to D_s^*(0^+)^+ \to D_s(0^-)\pi^+$ from the triality selection rules that Cartan's supersymmetry predicts[5, 6, 7].

We define a Dirac spinor composed of ψ and $\mathcal{C}\psi$

$$\begin{aligned}
\psi &= \xi_1 \boldsymbol{i} + \xi_2 \boldsymbol{j} + \xi_3 \boldsymbol{k} + \xi_4 \boldsymbol{I} \\
&= \begin{pmatrix} \xi_4 + i\xi_3 & i\xi_1 - \xi_2 \\ i\xi_1 + \xi_2 & \xi_4 - i\xi_3 \end{pmatrix} \\
\mathcal{C}\psi &= -\xi_{234}\boldsymbol{i} - \xi_{314}\boldsymbol{j} - \xi_{124}\boldsymbol{k} + \xi_{123}\boldsymbol{I} \\
&= \begin{pmatrix} \xi_{123} - i\xi_{124} & -i\xi_{234} + \xi_{314} \\ -i\xi_{234} - \xi_{314} & \xi_{123} + i\xi_{124} \end{pmatrix}
\end{aligned} \tag{2}$$

and another Dirac spinor composed of ϕ and $\mathcal{C}\phi$

$$\begin{aligned}
\phi &= \xi_{14} \boldsymbol{i} + \xi_{24} \boldsymbol{j} + \xi_{34} \boldsymbol{k} + \xi_0 \boldsymbol{I} \\
&= \begin{pmatrix} \xi_0 + i\xi_{34} & i\xi_{14} - \xi_{24} \\ i\xi_{14} + \xi_{24} & \xi_0 - i\xi_{34} \end{pmatrix} \\
\mathcal{C}\phi &= -\xi_{23}\boldsymbol{i} - \xi_{31}\boldsymbol{j} - \xi_{12}\boldsymbol{k} + \xi_{1234}\boldsymbol{I} \\
&= \begin{pmatrix} \xi_{1234} - i\xi_{12} & -i\xi_{23} + \xi_{31} \\ -i\xi_{23} - \xi_{31} & \xi_{1234} + i\xi_{12} \end{pmatrix}
\end{aligned} \tag{3}$$

which interact with four dimensional vector fields X.

The trilinear form of electromagnetic interaction in these bases is

$$\begin{aligned}
\mathcal{F} &= {}^t\phi \mathcal{C} X \psi = {}^t\phi \gamma_0 x^\mu \gamma_\mu \psi \\
&= x_1(\xi_{12}\xi_{314} - \xi_{31}\xi_{124} - \xi_{14}\xi_{123} + \xi_{1234}\xi_1) \\
&+ x_2(\xi_{23}\xi_{124} - \xi_{12}\xi_{234} - \xi_{24}\xi_{123} + \xi_{1234}\xi_2) \\
&+ x_3(\xi_{31}\xi_{234} - \xi_{23}\xi_{314} - \xi_{34}\xi_{123} + \xi_{1234}\xi_3) \\
&+ x_4(-\xi_{14}\xi_{234} - \xi_{24}\xi_{314} - \xi_{34}\xi_{124} + \xi_{1234}\xi_4) \\
&+ x_{1'}(-\xi_0\xi_{234} + \xi_{23}\xi_4 - \xi_{24}\xi_3 + \xi_{34}\xi_2) \\
&+ x_{2'}(-\xi_0\xi_{314} + \xi_{31}\xi_4 - \xi_{34}\xi_1 + \xi_{14}\xi_3) \\
&+ x_{3'}(-\xi_0\xi_{124} + \xi_{12}\xi_4 - \xi_{14}\xi_2 + \xi_{24}\xi_1) \\
&+ x_{4'}(\xi_0\xi_{123} - \xi_{23}\xi_1 - \xi_{31}\xi_2 - \xi_{12}\xi_3)
\end{aligned} \tag{4}$$

In the case of weak interaction, we replace the coupling $\gamma_0 x^\mu \gamma_\mu$ to $\gamma_0 x^\mu \gamma_\mu(1-\gamma_5)$ and try to make the couplings between fermions and vector particles become unified in the form

$$\sum_{i=1}^{4}(x_i \mathcal{C}\phi\,\mathcal{C}\psi + x_{i'}\mathcal{C}\phi\,\psi)$$

by suitable choice of 1 or $-\gamma_5$.

Except the term $x_{4'}\xi_0\xi_{123}$, which is $x_{i'}\phi\mathcal{C}\psi$ type, it is possible by the following choice

$$\begin{aligned}
\mathcal{G} &= x_1(\xi_{12}\xi_{314} - \xi_{31}\xi_{124} + \langle\xi_{14}\gamma_5\rangle\xi_{123} - \xi_{1234}\langle\gamma_5\xi_1\rangle) \\
&+ x_2(\xi_{23}\xi_{124} - \xi_{12}\xi_{234} + \langle\xi_{24}\gamma_5\rangle\xi_{123} - \xi_{1234}\langle\gamma_5\xi_2\rangle) \\
&+ x_3(\xi_{31}\xi_{234} - \xi_{23}\xi_{314} + \langle\xi_{34}\gamma_5\rangle\xi_{123} - \xi_{1234}\langle\gamma_5\xi_3\rangle) \\
&+ x_4(\langle\xi_{14}\gamma_5\rangle\xi_{234} + \langle\xi_{24}\gamma_5\rangle\xi_{314} + \langle\xi_{34}\gamma_5\rangle\xi_{124} - \xi_{1234}\langle\gamma_5\xi_4\rangle) \\
&+ x_{1'}(\langle\xi_0\gamma_5\rangle\xi_{234} + \xi_{23}\xi_4 - \xi_{24}\xi_3 + \langle-\xi_{34}\gamma_5\rangle\xi_2) \\
&+ x_{2'}(\langle\xi_0\gamma_5\rangle\xi_{314} + \xi_{31}\xi_4 - \xi_{34}\xi_1 + \langle-\xi_{14}\gamma_5\rangle\xi_3) \\
&+ x_{3'}(\langle\xi_0\gamma_5\rangle\xi_{124} + \xi_{12}\xi_4 - \xi_{14}\xi_2 + \langle-\xi_{24}\gamma_5\rangle\xi_1) \\
&+ x_{4'}(\xi_0\xi_{123} - \xi_{23}\xi_1 - \xi_{31}\xi_2 - \xi_{12}\xi_3).
\end{aligned} \tag{5}$$

We allow also direct channel couplings of ${}^t\phi\mathcal{C}x_4{}'\mathcal{C}\phi$ and ${}^t\psi x_4{}'\psi$.

Experimentally, violation of CP was observed in the decay of B^0 and B_s around 1997. In the case of $B \to K\pi$, there is a constraint on the unitarity angle γ, which is called Fleischer-Mannel bound by Grossmann et al[3, 4]. They derived the bound for the angle γ of unitary triangle, $\sin^2\gamma > R + 1.645\sigma_R$, with $R = 0.65 + / - 0.40$ and the uncertainty σ_R.

In comparison to $B \to K\pi$ decay, $B^0 \to K^0 J/\Psi$ contains weak final state interactions. In order to evaluate the $B^0 \to K^0 J/\Psi$ decay amplitudes we fix the initial configuration of $B^0 = d\bar{b}$ and the final configuration $K^0 = d\bar{s}$, $J/\Psi = c\bar{c}$, and a quark is expressed as a Dirac spinor ${}^t(\psi, \mathcal{C}\psi)$ and an anti-quark is expressed as a Dirac spinor ${}^t(\phi, \mathcal{C}\phi)$.

In penguin diagrams of $B^0 \to K^0 J/\Psi$, an anti-quark $\bar{b}$ emits a vector particle x_4' and transforms itself to a $\bar{c}$ quark, emits a vector particle x_4' that changes to a J/Ψ, and absorbs the vector particle and transforms itself to a $\bar{s}$ quark. Couplings of loops of a vector particle and an antiquark can be $1\,1$ type, shown in Fig.3 and $\gamma_5\gamma_5$ type, shown in Fig.4. We can combine the $\gamma_5\gamma_5$ and the $1\,1$ type to make the effective coupling $(1-\gamma_5)(1-\gamma_5)$ type.

In penguin diagrams of $\bar B^0 \to \bar K^0 J/\Psi$, a quark b emits a vector particle x_4' and transforms itself to a c quark, and emits a vector particle x_4' that changes to a J/Ψ, and absorbs the vector particle and transforms itself to an s quark. Couplings of a loop of vector particles and an antiquark can be $1\,1$ type, shown in Fig.5 and $\gamma_5\gamma_5$ type, shown in Fig.6. The coupling of a c quark and a vector particle x_4' is pseudoscalar, which we indicate by (ps).

The penguin diagrams of $\bar B^0 \to \bar K^0\, J/\Psi$ of $1\,1$ type are simple charge conjugation of $B^0 \to K^0\, J/\Psi$, but those of γ_5 type are different. Space components of the $\bar b$ quark in B^0 are small components of Dirac spinors, while those of the b quark in $\bar B^0$ are large components of spinors. It means that amplitudes of γ_5 contribution in $B^0 \to K^0\, J/\Psi$ are suppressed as compared to $\bar B^0 \to \bar K^0\, J/\Psi$.

In the $B^0 \to \bar K^0\, J/\Psi$ decay, there are tree diagrams of type I, in which vector particle of $c\bar c$ is emitted from $\bar b$, or tree diagrams of type II, in which a vector particle that decays to $c\bar s$ is emitter from $\bar s$, and after final state interactions J/Ψ and K^0 are created.

In the analysis of Coulomb interaction between electrons and holes using quaternion basis[12], it was necessary to make couplings of a photon x_4 to an electron and a photon $x_4{}'$ to electrons equivalent, for reproducing electron-hole interactions.

In the present case, couplings of a vector particle x_4' produced from a $\ell\bar\ell$ pair of J/Ψ to a $\bar q$ of $\bar B$, and couplings of a vector particle x_4 produced from a $q\bar q$ pair in J/Ψ and a $\bar q$ in K^0 are equivalent, and we can create a $\phi\gamma_5\mathcal{C}\psi$ or $\mathcal{C}\phi\gamma_5\psi$ vertex of x_4 from the source of x_4'. By the final state interaction, the created c and $\bar c$ interchanged from $\bar b$ in B^0 produce J/Ψ meson, and the created s quark and the original d quark of B^0 produce a $\bar K^0$ meson. In the evaluation of the matrix elements, we choose the original quark and the original anti-quarks are large components, if it is possible. The time component of the amplitude of $B^0 \to K^0\, J/\Psi$ and $\bar B^0 \to \bar{K^0}\, J/\psi$ of $\gamma_5\gamma_5$ type contains the small component ξ_{1234} and they are expected to be much smaller than those of the $1\,1$ type.

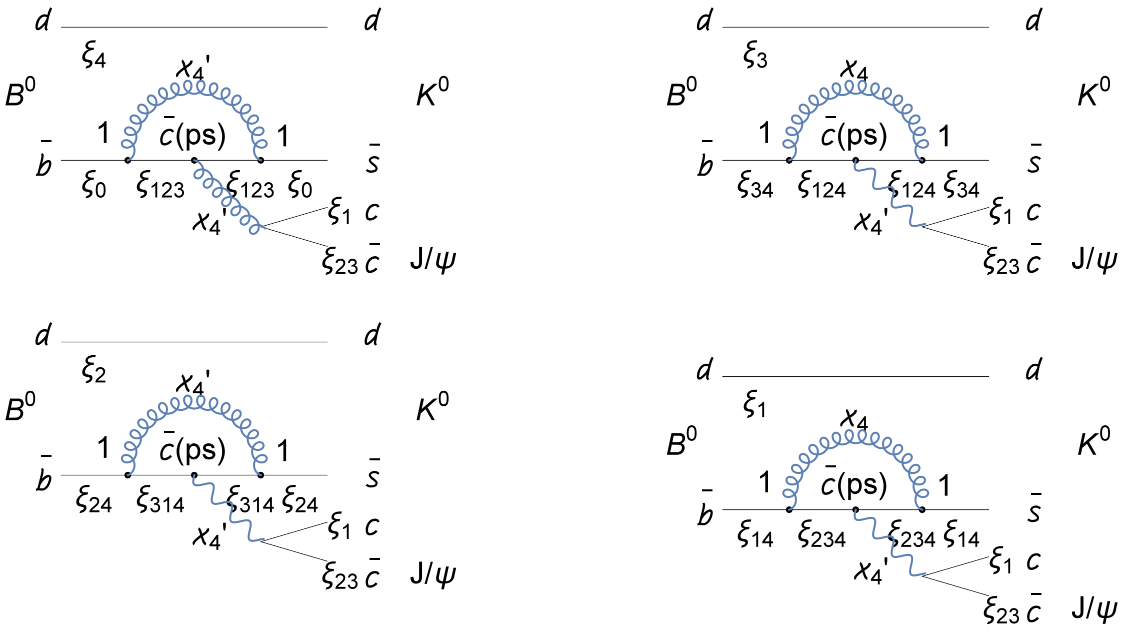

Figure 3: Typical diagrams of $B^0 \to K^0\, J/\Psi$ decay, penguin diagram 1 1 type. In the J/Ψ configurations, ${x_4}'$ decays to $\xi_1\xi_{23}$, $\xi_2\xi_{31}$ or $\xi_3\xi_{12}$.

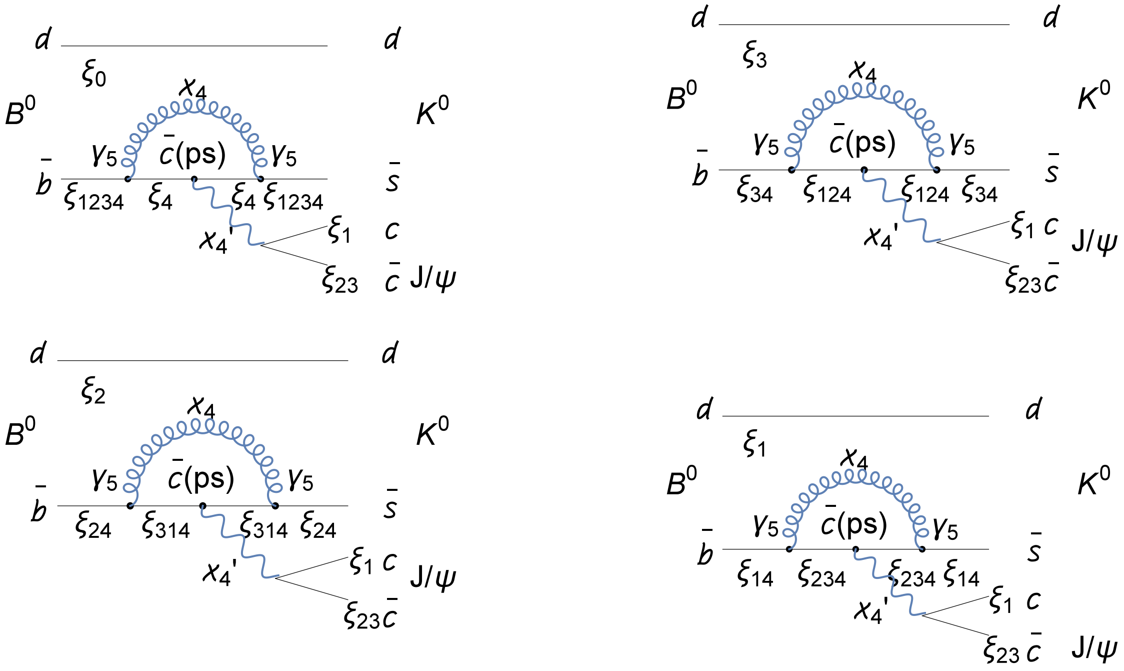

Figure 4: Typical diagrams of $B^0 \to K^0\, J/\Psi$ decay, penguin diagram $\gamma_5\gamma_5$ type. In the J/Ψ configurations, ${x_4}'$ decays to $\xi_1\xi_{23}$, $\xi_2\xi_{31}$ or $\xi_3\xi_{12}$.

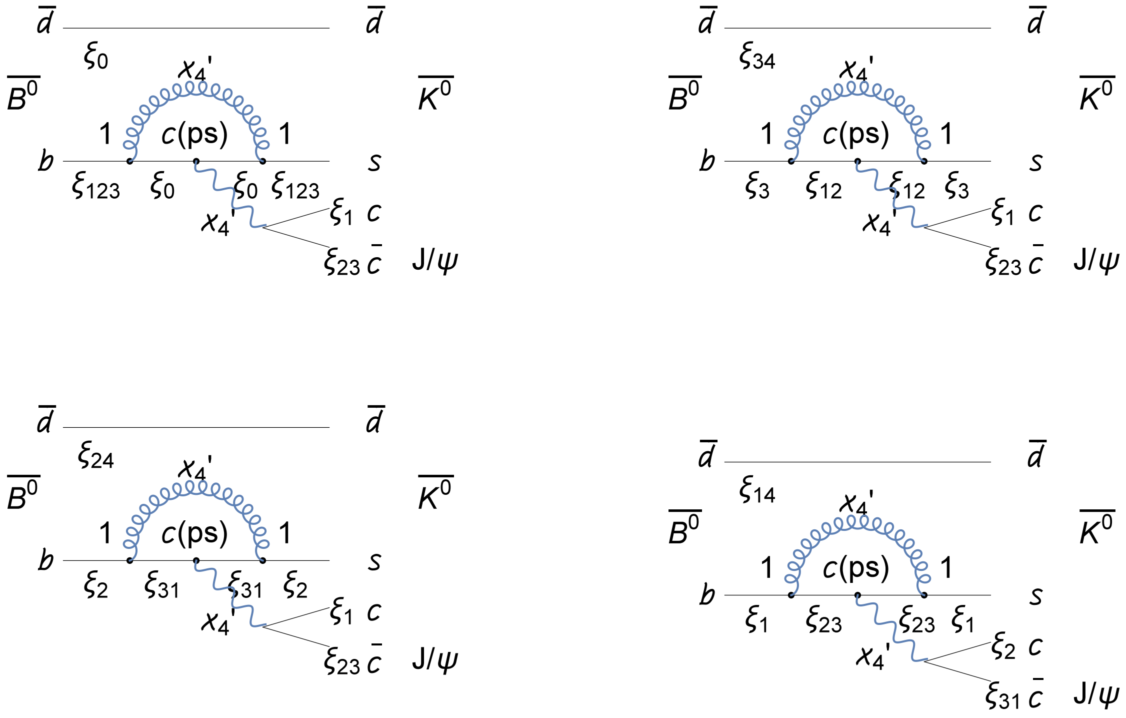

Figure 5: Typical diagrams of $\bar{B}^0 \to \bar{K}^0\, J/\Psi$ decay. penguin diagram 1 1 type. In the J/Ψ final states, a vector particle $x_4{}'$ decays to $\xi_1\xi_{23}$, $\xi_2\xi_{31}$ or $\xi_3\xi_{12}$.

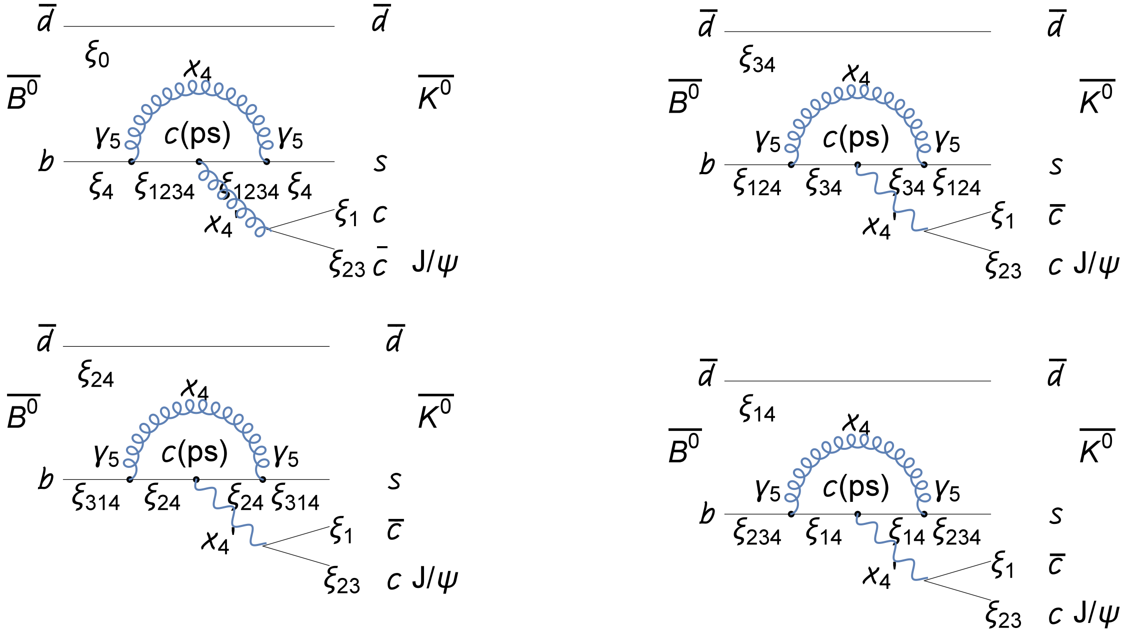

Figure 6: Typical diagrams of $\bar{B}^0 \to \bar{K}^0\, J/\Psi$ decay, penguin diagram $\gamma_5\gamma_5$ type. In the J/Ψ final state, $x_4{}'$ decays to $\xi_1\xi_{23}$, $\xi_2\xi_{31}$ or $\xi_3\xi_{12}$.

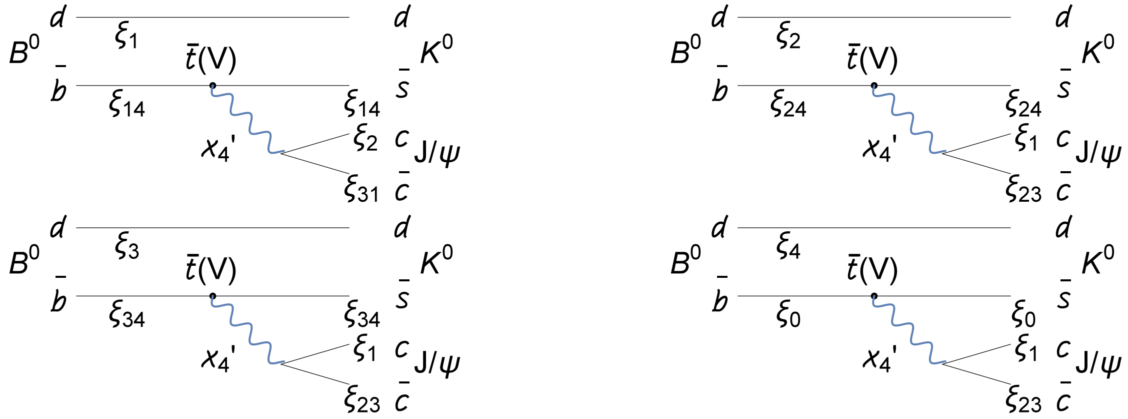

Figure 7: Tree diagrams of $B^0 \to K^0\, J/\Psi$ decay (type I). The J/Ψ is produced from the vector particle x'_4.

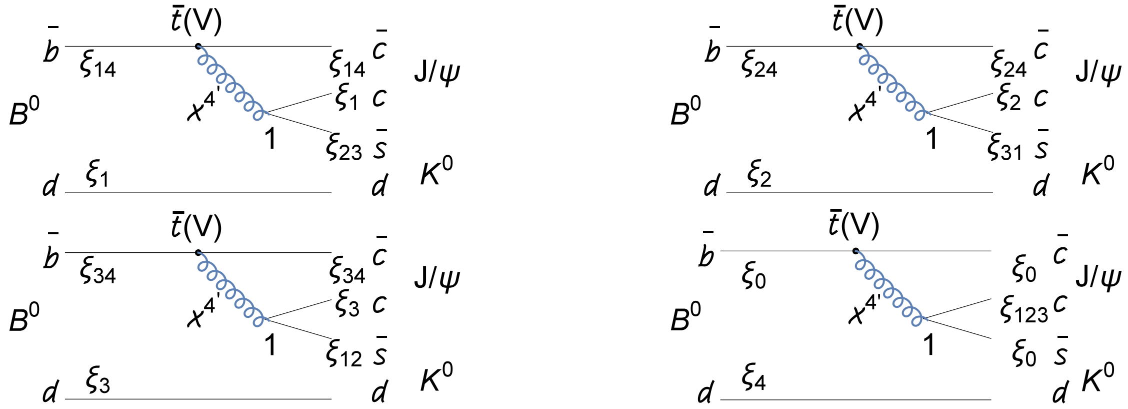

Figure 8: Tree diagrams of $B^0 \to K^0\, J/\Psi$ decay (type II). The J/Ψ is not produced from the vector particle x'_4.

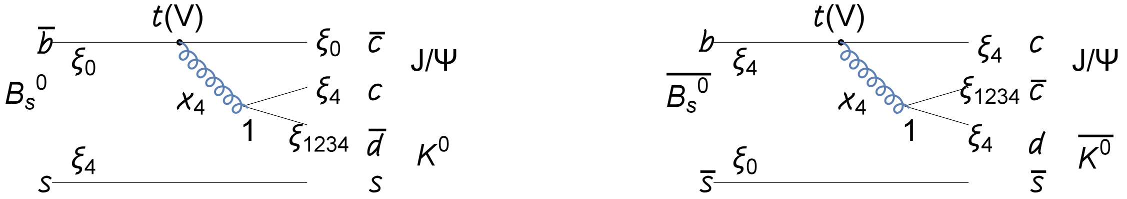

Figure 9: Typical tree diagrams of type II $B_s^0 \to K^0\, J/\Psi$ decay (left) and $\bar{B}_s^0 \to \bar{K}^0\, J/\Psi$ decay (right).

In the case of 1 1 type interactions, diagrams of type I is symmetric under charge conjugation, but diagrams of type II $B_s^0 \to K^0\, J/\Psi$ and $\bar{B}_s^0 \to \bar{K}^0\, J/\Psi$ as shown in Fig.9 are not symmetric. The 1 1 interaction of $B_s^0 \to K^0\, J/\Psi$, J/Ψ consists of $\bar{c}(\xi_0)c(\xi_4)$ and K^0 consists of $\bar{s}(\xi_{1234})d(\xi_4)$, i.e. K^0 has the small component ξ_{1234}, or the strength of the tree diagram of $c\bar{c}\,K^0$ becomes weak, same as in penguin diagram of $\gamma_5\gamma_5$ type and the number of difference of events $N_{\bar{B}_s^0} - N_{B_s^0}$ becomes large. In the case of space components of $B_s^0 \to K^0\, J/\Psi$, suppression of J/Ψ creation occurs, but it would be difficult to detect from experimental data of $c\bar{c}\,K^0$.

The 1 1 interaction of $\bar{B}_s^0 \to \bar{K}^0\, J/\Psi$, J/Ψ consists of $c(\xi_4)\bar{c}(\xi_{1234})$, and $\bar{K}^0$ consists of $d(\xi_4)\bar{s}(\xi_0)$, i.e. J/Ψ has the small component ξ_{1234}. Effects of this suppression on the strength of the $c\bar{c}\,\bar{K}^0$ may be difficult to detect, but in the case of the space components of $\bar{B}_s^0 \to \bar{K}^0\, J/\Psi$, suppression of $\bar{K}^0$ creation occurs, and becomes weak, same as in penguin diagrams of γ_5 type, and the number of difference of events $N_{\bar{B}_s^0} - N_{B_s^0}$ becomes small. The B^0 tags and the $\bar{B}^0$ tags in

The above properties are what the BABAR experiment of $c\bar{c}\,K_L^0$ of B^0 tags and $\bar{B}^0$ tags in the $\Delta t = t_{CP} - t_{flavor} > 0$ region show [2].

The experimental data of CP even final states [2] shows enhancements in raw CP asymmetry in $|\Delta t| \simeq 6$ps region. We expect this is the contribution of type II tree diagram generating $\bar{K}^0(s(\xi_4)\bar{d}(\xi_0))$, and that of $\gamma_5\,\gamma_5$ type penguin diagrams generating $\bar{K}^0(\bar{d}(\xi_0)s(\xi_4))$ which is stronger than $K^0(d(\xi_0)\bar{s}(\xi_{1234}))$.

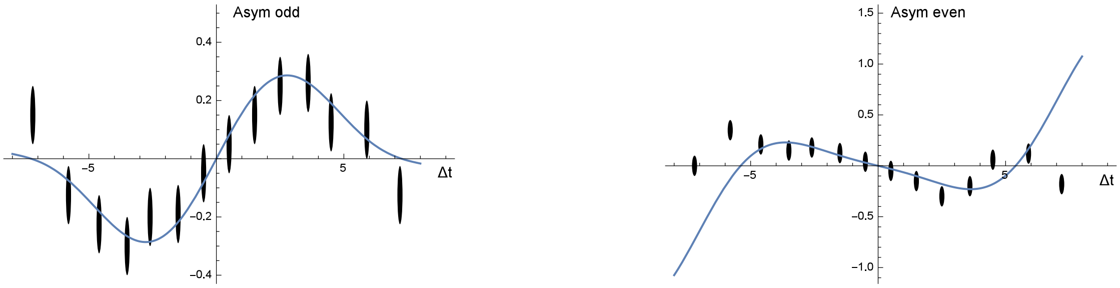

Figure 10: CP asymmetries in $B^0 \to J/\Psi K$ decay of CP-odd final state (left) and CP-even final state (right).

In our B decay to $J/\Psi K$, the CP-odd final state of [2] can be approximated by

$$\begin{aligned}
&(e^{(t-1)/16}[1+\cos[\Delta m_B(t-2)]])^2 - (e^{-(t+1)/16}(1+\cos[\Delta m_B(t+2)]))^2 \\
&= e^{(t-1)/8} 4\cos^4\frac{\Delta m_B(t-2)}{2} - e^{-(t+1)/8} 4\cos^4\frac{\Delta m_B(t+2)}{2}
\end{aligned} \tag{6}$$

and CP-even final state of [2] can be approximated by

$$\begin{aligned}
&\frac{1}{8}(e^{(t-1)/16}(1-\cos[\Delta m_B(t-2)]))^2 - \frac{1}{8}(e^{-(t+1)/16}(1-\cos[\Delta m_B(t+2)]))^2 \\
&= e^{(t-1)/8}\frac{1}{2}\sin^4\frac{\Delta m_B(t-2)}{2} - e^{-(t+1)/8}\frac{1}{2}\sin^4\frac{\Delta m_B(t+2)}{2}
\end{aligned} \tag{7}$$

where $\Delta m_B = 0.463\mathrm{ps}^{-1}$ is fixed[4], which are shown in Fig.10. Center of an elliptic disk is that of an experimental point, and the error bar of the asymmetrys are fixed to 0.2, and the ratio of error bars in asymmetry axis and in Δt axis is fixed to the goldenratio $(1+\sqrt{5})/2$ which ratio is the value used in Mathematica for presentations of asymmetry curves.

We expect that the experimental asymmetry of $B^0 \to K^0\, J/\Psi$ and $\bar{B}^0 \to \bar{K}^0\, J/\Psi$ at large Δt can be understood from the final state wave functions caused by the $1-\gamma_5$ vertexes.

3 B^0 decay into D^+D^- and B_s^0 decay into $D_s^+D_s^-$

Cartan's supersymmetry based on Clifford algebra presents large asymmetry between the weak decay of fermions ψ_L and $\mathcal{C}\phi_L$. The origin of the discrepancy between the raw asymmetry of CP even final states $J/\Psi K_L^0$ and the best fit projection in Δt of B^0 tagged events and $\bar{B}^0$ tagged events[2] is expected to be due to the $\gamma_5\gamma_5$ type penguin interaction. One can ask whether similar effects can be seen in other decay processes leading to different final states.

There are analysis of CP symmetry in $B^0 \to J/\Psi K^0_S$, $B^0 \to D^-D^+$ and $B^0_s \to D^-_s D^+_s$[14]. In the analysis of $B^0 \to J/\Psi K^0_S$, penguin diagrams of γ_5 were not included and the CP asymmetry was not observed. Results of $B^0 \to J/\Psi K^0_S$[14, 15, 16] is less clear than that of $B^0 \to J/\Psi K^0_L$.

In the penguin diagram of $B^0 \to J/\Psi \bar{K}^0$, the vector particle $c\bar{c}$ emitted from the anti-quark transformed to J/Ψ, while in the case of $B^0 \to D^+D^-$, the c is absorbed in D^- and $\bar{c}$ is absorbed in D^+. There is not large differences in penguin diagrams and tree diagrams, and clear CP asymmetry was not observed. An experiment of $B^0 \to D^{(*)}\bar{D^{(*)}}$ using partial reconstruction of $B^0 \to D^{*-}X\ell^+\nu_\ell$ and a kaon tag[18] does not show clean CP asymmetry.

4 Discussion and conclusion

We applied Cartan's supersymmetry to weak interaction and analyzed the $B^0 \to K^0\, J/\Psi$ and $B^0 \to D^-_d D^+_d$ and $B^0_s \to D^+_s D^-_s$ decay using vector particles x_i and x'_i $(i = 1, 2, 3, 4)$ and assigning couplings to quarks by $1 - \gamma_5$ vertices, and inducing effective couplings of W bosons, Z bosons and photons.

We observed that the CP symmetry of $B^0 \to K^0_L J/\Psi$ is violated, while that of $B^0 \to D^-_d D^+_d$ and $B^0_s \to D^-_s D^+_s$ are not strongly violated. In these decay processes, there appear penguin diagrams and tree diagrams, and in the CP asymmetry of $B^0 \to K^0_L J/\Psi$ and $\bar{B}^0 \to \bar{K}^0_L J/\Psi$, space components of penguin diagrams of $\gamma_5\gamma_5$ type and the time component of tree diagrams of γ_5 type play important roles in changing the strength of $c\bar{c}\,K^0$ events and $c\bar{c}\,\bar{K}^0$ events, where $c\bar{c}$ is not necessarily the J/Ψ state.

We showed that Cartan's supersymmetry is a useful tool for analyzing violation of CP symmetry of $B^0, \bar{B}^0$ and $B^0_s, \bar{B}^0_s$ systems. Difficulties in choosing appropriate CKM ampli-

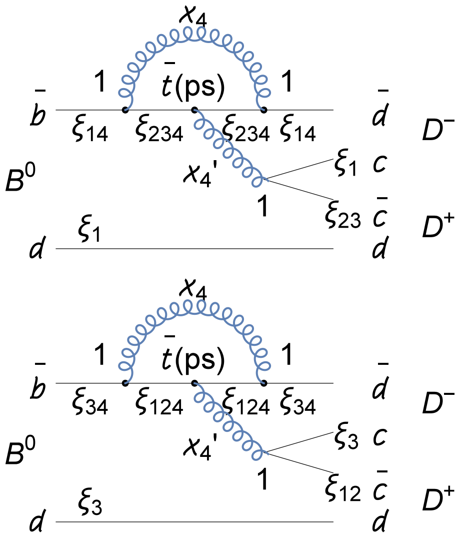

Figure 11: Penguin diagrams of $B^0 \to D^- D^+$ decay.

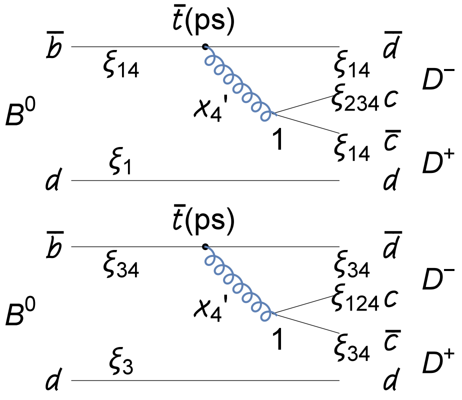

Figure 12: Tree diagrams of $B^0 \to D^- D^+$ decay.

tudes V_{cs}, V_{cb} and V_{cd} that explain $B \to \ell\bar{\ell}$ and $B_s \to \ell\bar{\ell}$ consistently can be removed by an appropriate assignment of the strength of penguin diagram amplitudes and tree diagram amplitudes [19].

References

[1] J. Bernabeu and F. Martinez-Vidal, *Colloquium*: Time-reversal violation with quantum-entangled B mesons, Rev. Mod. Phys.**87** (2015) 165-182.

[2] B. Aubert et al, (BABAR collaboration), Phys. Rev. D**79** (2009) 072009; arXiv:0902.1708v2[hep-ex]

[3] R. Fleischer and T. Mannel, Constraining the CKM angle γ and penguin contributions through combined $B \to \pi K$ branching ratios, [hep-ph/9704423].

[4] Y. Grossman, Y. Nir, S. Plaszezynski and M-H. Schune, Implication of the Fleisher-Mannel Bound, [hep-ph/9709288 v1].

[5] É. Cartan, *La théorie des spineurs* (1937), *The theory of Spinors*, Dover Pub. (1966) p.118.

[6] S. Furui, Fermion Flavors in Quaternion Basis and Infrared QCD, Few Body Syst. **52**, (2012) 171-187, [hep-ph/1104.1225].

[7] S. Furui, Triality selection rules of Octonion and Quantum Mechanics, [hep-ph/1409.3761].

[8] S.Furui, Cartan's Supersymmetry and Weak and Electromagnetic Interactions, [hep-ph/1502.04524]

[9] S. Furui, Cartan's Supersymmetry and the Decay of a $H^0(0^+)$, [hep-ph/1504.03795].

[10] M. Zeller, Particle Decays Point an Arrow of Time, Physica **5** (2012) 129-130.

[11] P. Becher, M, Böhm and H. Joos, *Eichtheorien*, Teubener Studienbücher (1981) p.347.

[12] S. Furui and T. Takano, On the Amplitude of External Perturbation and Chaos via Devil's Staircase - Stability of Attractors -, submitted to Nonlinear Dynamics; arXiv:1312.3991[nlin.CD]

[13] S. Furui, Cartan's Supersymmetry and the Decay of $H^0(0^+, 125\mathrm{GeV})$ to $\gamma\gamma, WW$ and ZZ, Abstract of FPCP2015, Nagoya University (2015).

[14] R. Fleischer, Extracting γ from $B_{s(d)} \to J/\Psi K_S$ and $B_{d(s)} \to D^+_{d(s)} D^-_{d(s)}$, hep-ph/9903455.

[15] K. De Bruyn and R. Fleischer, A Roadmap to Cintrol Penguin Effects in $B^0_d \to J/\psi\, K^0_S$ and $B^0_s \to J/\psi\, \phi$, 1412.06834 v3 [hep-ph].

[16] R. Fleischer, Towards new frontiers in CP violation in B decays, Journal of Physics: Conference Series **556** (2014) 012035, IOP Publishing.

[17] B. Aubert et al, (BABAR collaboration), Direct CP asymmetry in $B^0 \to K^+\pi^-$ decays, Phys. Rev. Lett.**93** (2004) 131801.

[18] J.P. Lees et al, (BABAR collaboration), Search for CP Violation in $B-0-\bar{B}^0$ Mixing Using Partial Reconstruction of $B^0 \to D^{*-}X\ell^+\nu_\ell$ and a Kaon Tag, Phys. Rev. Lett.**111** (2013) 101802.

[19] S. Furui, Departure from the Standard Model of Meson Decays and Cartan's Supersymmetry, arXiv:1511.07774[physics.ge-ph].